



Harmonically driven slider: Markovian dynamics between two limiting attractors

D. Maza*, J.M. Schins

Departamento de Física y Matemática Aplicada, Facultad de Ciencias, Universidad de Navarra, Pamplona, Spain

ARTICLE INFO

Article history:

Received 13 November 2018

Revised 18 December 2018

Accepted 18 December 2018

Keywords:

Tribology

Non-linear dynamics

Stochastic models

ABSTRACT

We present experimental data of the motion of a cylindrical slider interacting only by friction with a polished horizontal tray. The tray is harmonically shaken in the horizontal direction. Below a certain threshold of the driver acceleration, the slider permanently sticks to its substrate due to the static friction. Above that threshold, the observed slider dynamics is periodic (synchronous with the driver oscillation frequency) but not wholly harmonic: for driver accelerations little beyond the threshold, the slider velocity signal is quasi-triangular. A Markovian model shows that, with increasing driver acceleration, the slider motion increasingly tends to be harmonic again, though with a prominent phase difference respect to the driver.

© 2019 Elsevier Ltd. All rights reserved.

1. Introduction

The established laws of sliding friction were discovered by Leonardo da Vinci in 1493, a pioneer in tribology, but the correlations documented in his notebooks were not ever published [1]. Those ideas became only recently known as being identical to those of Guillaume Amontons published in 1699 [2], and that laws that Coulomb published in 1821 [3]. In 1750 Leonhard Euler derived the angle of repose of a weight on an inclined plane and first distinguished between static and dynamic friction. Ever since increasingly sophisticated models of friction have been published, each successful for the particular domain where they are applied. Today many tribologists believe that long-range attractive isotropic Van der Waals forces cause dynamic friction, and shorter-range attractive anisotropic Van der Waals forces, static friction [4].

Despite the microscopic peculiarities of solid-solid surface interaction, the complex dynamics observed in a large variety of mechanical devices can be retrieved from just a few macroscopic quantities. The dynamic effects include stick-slip transitions, regular and chaotic self-oscillations, as they were discussed by Popp and Stelzer in 1990 [5]. After their seminal paper a large number of works have been devoted to understanding the interplay between the static and dynamic friction coefficients, μ_{stat} and μ_{dyn} respectively, on the resulting dynamics of excited frictional systems [6]. A possibly superfluous effect to mention is that the response of the slider changes from period to period. No two periods are identical.

This is solid experimental proof that, whatever the interplay between the two friction coefficients, it cannot be possibly deterministic on the mesoscopic scale. Hence, theoretical friction modeling of dry surfaces must necessarily be of a probabilistic kind.

Fig. 1a summarizes some of the most common deterministic models representing frictional interaction. In the sketch, the magnitude of friction force F_f is represented against the relative velocity between the moving objects, v . The four models are all deterministic. The piecewise line represents the standard Coulombic model: the friction force starts out at zero, and instantaneously rises to the dynamic friction level, with a delta function at time zero. The red line represents the smooth friction interaction, and rises linearly in time until it intersects, upon exiting the grey area, the dynamic force level. The blue curve represents Bensons static model: it starts out at zero, too, jumps instantaneously to the static force level $F_{stat} = \mu_{stat}Mg$, and relaxes exponentially to the dynamic force level $F_{dyn} = \mu_{dyn}Mg$, where M stands for the sliders mass. Finally, the green curve represents Bensons velocity-dependent friction model (see [7] for a more detailed explanation). More sophisticated approaches have been developed to include a large variety of parameters, like humidity, temperature, and whatever macroscopic experimental-physical quantity [8]. The function we use in our work offers the same options. It is not depicted in the schematic because it is a fundamentally different function: it has two arguments instead of one. The second argument is the drivers harmonic phase: as we use setup (c), an inert mass is harmonically shaken in a horizontal direction. In the laboratory frame, the force function is the linear extrapolation of Bensons velocity-dependent function, until the line hits the static force; its phase is zero throughout, meaning that the slider is like glued to the

* Corresponding author.

E-mail address: dmaza@unav.es (D. Maza).

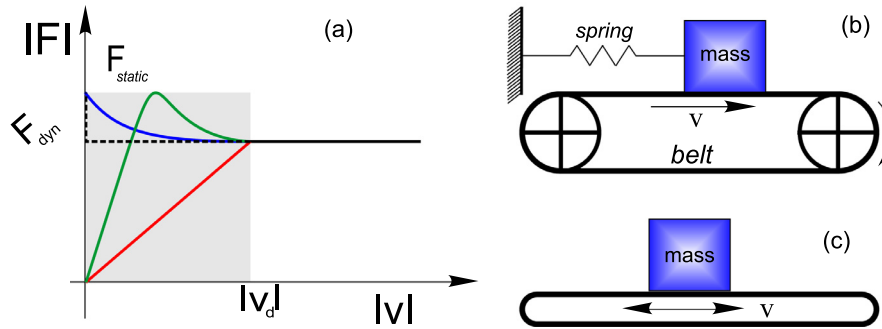


Fig. 1. Commonly used models of dry friction and experimental setups: (a) Dry friction models, described in more detail below; (b) Typical experimental setup used to measure the dynamic friction coefficient. (c) Sketch of the experimental setups introduced in this work. Note that the slider moves freely, only under the action of alternating frictional force.

moving substrate. For higher velocities, the force reduces to the dynamic force level, though with an increasing phase delay with respect to the driver. At these higher driver velocities, the friction force performs a Markovian random walk, such that the sliders velocity always finds itself between two extremes which we had hysteresis attractor curves. The zero phase straight line to the static force level is the low-velocity attractor, and a second curve from the static force level back to the dynamic force level (joining at infinite velocities) is the other. For high enough accelerations, the friction force coincides with the second attractor. The “gray region” marks the velocity region where the models differ most. Our model differs from all other models in the Markovian aspect: only the two predetermined attractors (magnitude and phase) can be depicted, not the actual friction force.

Apart from the peculiar nature of the (inherently probabilistic) model, the experimental approach is peculiar, too. One of the reasons is that many of the used experimental setups are inspired by the industrial or applied process, like the effects of a cutting machine on a rotating piece or the induced chord self-vibrations by a violin bow. The canonical example of this type of devices regards the observed dynamics in the experiment sketched in Fig. 1b, where the competition between a controlled external force and the induced frictional interaction of the contact surfaces [9] results in complex, even random, movements.

The probabilistic element regarding this randomness is not of fundamental kind, like quantum indeterminacy, but rather of

the many-particle kind in Boltzmann classical thermodynamics: it trades in useless, $6N$ (positions and velocities of N particles at all times) knowledge of a single deterministic system for a few thermodynamic potentials and their arguments valid for infinite-ensemble averages. In a future experiment, we hope to be able to take up Feynman’s challenge, who claimed, “with dry metals it is very hard to show any difference” (between the friction coefficients) [10].

In this work, we introduce an elemental experimental setup, developed to analyze the dynamics of a dry slider-substrate system excited only by frictional forces. Instead of applying a continuous excitation like the one introduced in Fig. 1b, we apply a harmonic force to an *entirely* free mass that moves only under the action of friction and inertia, Fig. 1c. Then, the relative positions of driver and slider are analyzed and the origin of the slider dynamics is discussed.

2. Experimental setup

The apparatus used to perform the experiments is presented in Fig. 2. The setup consists of a horizontal tray (carefully leveled at ± 0.001 rad) with a bottom of uncoated glass flat windows (Edmund Scientific $102 \times 152 \times 2.4$ mm). The photograph region corresponds to a rectangular area of 80×40 mm. The tray is directly fastened to an electromechanical shaker (Tira TV52120), which defines the longitudinal axis, x off the setup. The perpen-

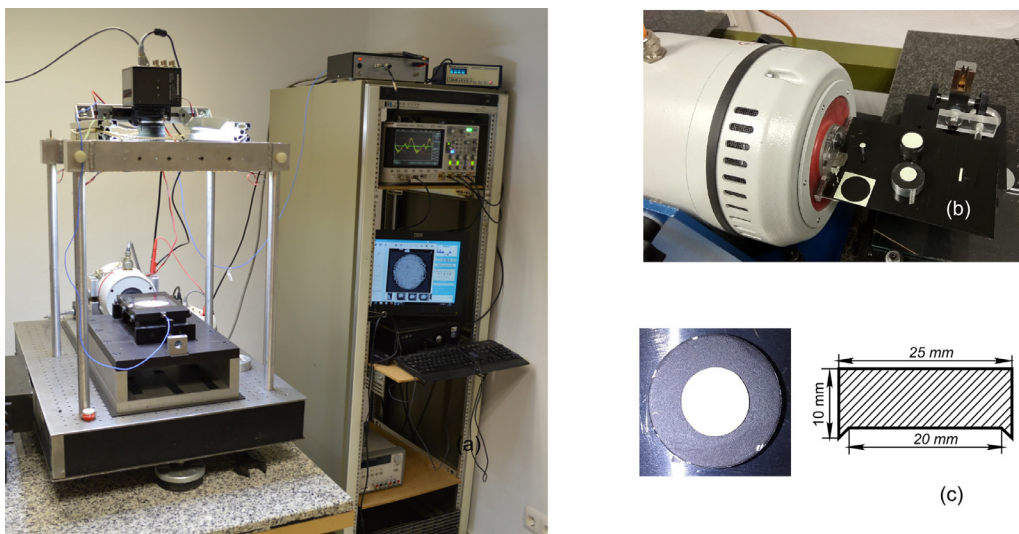


Fig. 2. Experimental devices: (a) Experimental setup used to analyze the slider dynamics. (b) A more simple and compact version of the same setup where it is possible to distinguish both slider and tray reference (see text for details). (c) Upper image and cut view of the slider.

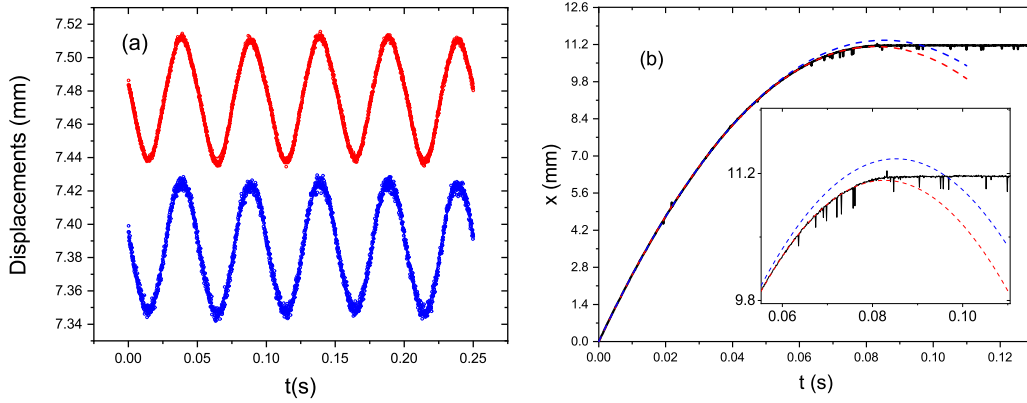


Fig. 3. Harmonic regime: (a) Temporal evolution of the tray (red dots) and the slider (blue dots) for $v_d\omega < \mu_{stat}g$ frame-lab referenced. The slider is permanently stuck to the substrate. Continuous lines are the harmonic fits of the experimental points. (b) Spatio-temporal evolution of the slider decelerating on a substrate at rest (continuous line). Two fits (dotted lines) differing four part in thousands are included to highlight the strong influence on the arrest dynamics of the dynamical friction coefficient. The inset is included to highlight the fit sensitivity to the μ_{dyn} small variation. (For interpretation of the references to color in this figure legend, the reader is referred to the web version of this article.)

dicular axis (y) in the horizontal plane is called transverse, and the out-of plane axis the vertical, z . Non-longitudinal displacements are minimized due to a couple of bearing guides placed at both side of the tray. The shaker is driven by a signal generator (Keithley 33220A) yielding high quality sinusoidal oscillations. A 3D-piezoelectric accelerometer, connected to the tray, measures the three axis accelerations. The slider is a rimmed, aluminum cylinder of 1 cm height, and 2.5 cm diameter (Fig. 2c). The mass of the slider is 21.19 ± 0.01 g. The rim at the cylinders bottom is carefully polished using high-grade paper sheets and polish liquid.

The drivers reference consists of a small-radius cylinder (with the same 1 cm height as the slider) glued onto the substrate and with a fluorescent disk on top of it. A homogeneous and incoherent light source allows for a zenithal high-speed camera (FASTCAM Mini UX100 - Photron) to record the positions of both slider and substrate in a single shot. The centroid of the photographed disks is calculated using an in-house developed image toolbox. The spatial resolution is as small as 80 μ m corresponding to the pixel size in the horizontal plane. Higher spatial resolution is possible at the cost of a lower temporal resolution.

The control parameter is the maximum tray acceleration, $v_d\omega$, with v_d the drivers velocity amplitude, and ω the drivers oscillation frequency. In order to explore a wide range of amplitudes with a minimum of shaker-induced noise, 20 Hz turned out to be the optimum driving frequency. Fig. 3a shows that, for $v_d\omega < \mu_{stat}g$, the slider is permanently stuck to the substrate. Beyond a certain threshold, the sticking process becomes a short-lived phenomenon. It only happens when the velocities of the slider and substrate are identical along a certain fraction of the oscillation period. For this reason, the drivers harmonic velocity will be considered the “attractive solution” of the sliders dynamics in the next paragraphs.

3. Experimental results

3.1. Uniform decelerating regime

Fig. 3a shows the slider moves jointly with the tray for smalls tray velocities. These dynamics occur when the tray acceleration is smaller than a certain threshold imposed by the static friction coefficient, μ_{stat} . In order to estimate the magnitude of the static and dynamics friction coefficients we first explore the uniform decelerating regime just by kicking the slider on the tray at rest, Fig. 3b. The measured trajectory is displayed by the continuous curve whereas dotted curves are numerical fits assuming a stick-free trajectory. Both fits differ only in four-part in one thousand

highlighting the sensitivity of this magnitude on the transition threshold to the stuck position. Thus, the second time derivative of the experimental data yields a good estimation of the dynamic friction coefficient, $\mu_{dyn} = 0.32 \pm 0.01$. However, despite the high spatiotemporal resolution reached by our experimental setup, the method is not able to give an objective approximation of μ_{stat} .

3.2. Harmonic frictional perturbation

We have just seen that, for $v_d\omega < \mu_{stat}g$, the slider is permanently stuck to the substrate (Fig. 3a). Upon gently increasing the oscillation amplitude, a smooth transition to a sliding regime could be expected. Yet, such a smooth transition does not exist. Instead, when the tray acceleration approaches to certain critical value, the slider starts to move at an unpredictable driver amplitude. Once it moves, it moves quasi-harmonically, out of phase with the driver as is displayed in Fig. 4. Quite notably, from the critical acceleration value upward, the sliders amplitude of motion does not increase smoothly from zero upwards, but it sets in at a non-zero value, proportional to the difference in friction coefficients.

The non-harmonicity of the slider motion is better visible in its velocity than in its position. An average over 18 periods reduces the noise. A further noise-reduction step was applied by passing the slider velocity through a lowpass filter with small bandwidth. As expected, the substrate velocity remains a pure harmonic, with amplitude v_d . Instead, the slider velocity is closer to a triangle with a slightly lower amplitude (see Fig. 7b).

4. Linear kernel convolution based on momentum transfer

In order to understand the origin of the slider kinematic features we implement an approach based on elemental kinematic assumptions. As the sliders velocity results from a continuously changing force operating on it, we assume that the slider dynamics is given by the convolution of the drivers speed with specific sliders deceleration kernel, $K_{slider}(t)$. Such kernel is equal to the sliders linearly decreasing velocity on a steady substrate divided by its integral. The kernel has inverse time units by definition. As the convolution integral is over time, the convolution has the same units as the drivers velocity. Hence, the sliders harmonic velocity response reads:

$$v_{harmonic}(t) = \int_{-\infty}^{\infty} ds K_{slider}(s)v_{driver}(t-s) \quad (1)$$

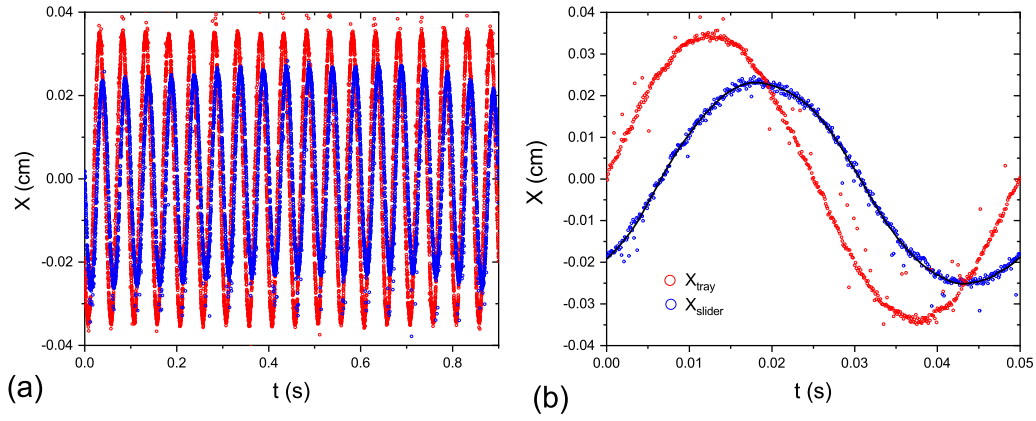


Fig. 4. Slider dynamics: (a) Detrended coordinates of the tray (red dots) and slider (blue dot) beyond the sliding threshold. (b) A single period of tray oscillation is zoomed and compared with the slider displacement. (For interpretation of the references to color in this figure legend, the reader is referred to the web version of this article.)

with the kernel K_{slider} defined as

$$K_{slider}(t) \equiv \frac{v_{deceleration}(t)}{\int_{-\infty}^{\infty} ds v_{deceleration}(s)} \quad (2)$$

Whatever the functional form of the Kernel, the sliders velocity response is always a harmonic signal, because the driver is harmonic. Hence, a convolution can describe the second attractor (the first one being the drivers velocity). To state the same in negative term: a convolution with a harmonic driver can never describe a non-harmonic signal. Yet our measured response data are clearly not harmonic. The physical reason of the convolutions failure to reproduce the slider dynamics close to the critical driver acceleration (where it equals $\mu_{stat}g$) is that the convolution ignores the role of the static friction coefficient, which controls, in fact, the transition between the stuck and stick-free dynamics, corresponding to the first and second attractor, respectively. None of the classical friction models, sketched in Fig. 1a, incorporates the experimentally obvious indeterminism inherent in the slider velocity, and none of them considers the slider motion as a competition between two harmonic attractors. In this sense the here presented approach breaks with the known standards.

The simplest model assumes a constant deceleration, whence a linearly decreasing deceleration velocity as a function of time. Consequently, the Kernel can be written as a function of one parameter only, the time during which the past forces have been operating on the slider, t_{mx} :

$$K_{slider}(t|t_{mx}) = \frac{2}{t_{mx}} \left(1 - \frac{t}{t_{mx}}\right) \theta(t) \theta(t_{mx} - t) \quad (3)$$

The Heaviside function is defined as usual: $\theta(t) = \begin{cases} 1 & \text{for } t \geq 0 \\ 0 & \text{for } t < 0 \end{cases}$, and the kernel satisfies the normalization condition:

$$\int_{-\infty}^{\infty} dt K_{kick}(t|t_{mx}) = 1 \quad (4)$$

This property of the kernel, combined with its finite duration t_{mx} implies that when $t_{mx} \rightarrow 0$, the kernel turns into a delta function. In that limit, the convolution response of the slider falls on top of the driver: the slider is “permanently stuck” to the substrate. The predicted “stick-free” velocity, v_{sf} is obtained from the expression:

$$\begin{aligned} v_{sf}(t|t_{mx}) &= \frac{2}{t_{mx}} \int_0^{t_{mx}} ds \left(1 - \frac{s}{t_{mx}}\right) v_d \cos \omega_0(t - s) \\ &= \frac{2v_d}{(\omega_0 t_{mx})^2} A_s \cos(\omega_0 t - \Delta\phi) \end{aligned} \quad (5)$$

with the definitions:

$$\left\{ \begin{aligned} A_s &\equiv \sqrt{A_a^2 + A_b^2} \\ \tan \Delta\phi &\equiv \frac{A_b}{A_a} \end{aligned} \right\} \left\{ \begin{aligned} A_a &\equiv 1 - \cos \omega_0 t_{mx} \\ A_b &\equiv \omega_0 t_{mx} - \sin \omega_0 t_{mx} \end{aligned} \right\} \quad (6)$$

Accordingly, the resulting slider maximum velocity and phase-delay against the tray signal can be predicted using an ordinary harmonic convolution, i.e. by plotting Eq. (6) as a function of the flight time t_{mx} . Fig. 5b represents the slider’s amplitude divided by the driver’s: it is always below unity due to energy conservation. Fig. 5a shows the phase delay of the slider with respect to

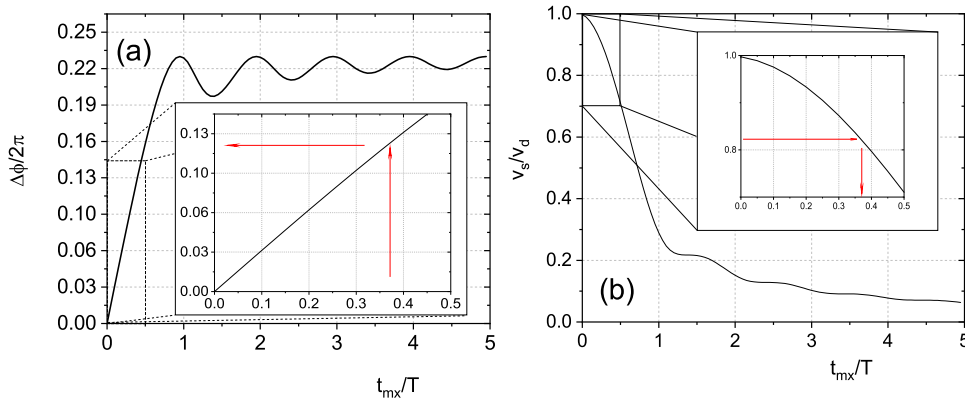


Fig. 5. Sliding regime: (a) Phase difference and velocity ratio, (b), between tray and slider obtained from the linear kernel convolution procedure. Insets: the measured ratio between $\frac{v_s}{v_d}$ (red arrows) provides a good estimation of t_{mx} as is possible to check from the expected phase difference determined in the inset of (a) (see text for details). (For interpretation of the references to color in this figure legend, the reader is referred to the web version of this article.)

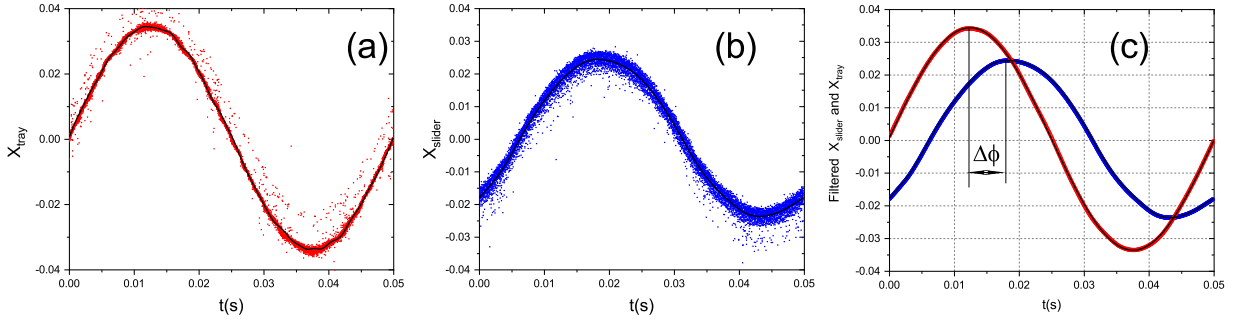


Fig. 6. Smoothed experimental results: The complete temporal signal displacements of tray, (a), and slider, (b), have been collapsed into a single period to obtain smoothed signals where the phase difference, $\Delta\Phi$, can be obtained (c).

the driver. Note that when the t_{mx} becomes larger than the oscillation time, T , the slider velocity tends to zero as is expected when the friction tends to disappear. As the time t_{mx} could be estimated from the phase-shift between tray and slider position signals (see Fig. 6c) we can use this magnitude to calculate the slider to tray velocity ratio, v_s/v_d as is sketched by the arrows in the insets of Fig. 5. Finally, the relation $\mu_{dyn}gt_{mx} = |v_d|$ allows for straightforward determination of t_{mx} from the data, as the dynamic friction coefficient and the driver amplitude are both known.

5. Discrete-Markovian walk model

Fig. 7 illustrates the gist of our model results. Fig. 7a shows only idealized data: the two harmonic attractor curves, corresponding to the static and dynamical solution of the convolution procedure, and the velocity signal calculated from the Markovian model. Fig. 7b shows only measured data: the driver and slider velocities averaged over heighten periods and finally, Fig. 7c shows a comparison of the measured and calculated slider velocities using the Markovian model. The latter will be explained in detail below.

Inspired in previous works that take into account the random character of the frictional interaction [11,12], we speculate that the driver velocity and the convolution solution act as competing attractors for the sliders dynamics.

The model needs to have the following limiting characteristics. Whenever the sliders and drivers velocities and accelerations are close enough, the slider should stick to the driver, and follow the first attractor. On the other hand, whenever the sliders and drivers velocities and accelerations are distant enough, the slider should follow the second, or stick-free attractor.

The basic idea of the Markovian propagation is to calculate the velocity of the slider from its previous velocity by means of a random generator. Here, the adjective previous refers to the temporal

discretization. We implement the randomness by defining a probability for the slider to move toward one attractor or the other, depending on whether the fraction of friction parameters is larger or smaller than that random number. For this reason, every single run of the code over one driver period gives slightly different results.

The propagation of the Markovian model makes use of three typical discrete functions:

1. the function “rnd[arg]”, which rounds off its real argument to the nearest integer;
2. the function “ran”, which yields a random number between zero and one;
3. the function “sgn[arg]”, which yields the values -1 or +1 depending on the sign of its argument.

These functions are crucial because, in discretizing the velocity to natural numbers n_j , the scaled velocity difference $\Delta n_j \equiv n_{j+1} - n_j$ should be a natural number, too. Apart from the random velocity numbers n_j , we also need to define the two attractors, which are fixed harmonics: the first (stuck to the driver) attractor is represented by the discretized velocity number n_{j+1}^{dr} , and the second (stick-free) attractor by the velocity number n_{j+1}^{sf} . In terms of the above functions, the Markovian velocity propagator reads

$$\Delta n_j \equiv \theta [\chi - \text{ran}] \text{sgn}[n_{j+1}^{dr} - n_j] + \text{rnd}[\chi] \theta [\text{ran} - \chi] \text{sgn}[n_{j+1}^{sf} - n_j] \quad (7)$$

where χ is a function of $\chi_\mu \equiv \frac{\Delta\mu}{\mu_{stat}}$ and $\chi_{acc} \equiv \frac{v_d\omega}{g}$. The former is a measure for the ratio of the friction coefficients, and the latter for the amplitude of the driver acceleration; and we also introduced the friction difference $\Delta\mu \equiv \mu_{stat} - \mu_{dyn}$. In the most simple of cases, χ is their direct product function: $\chi = \chi_\mu \chi_{acc}$.

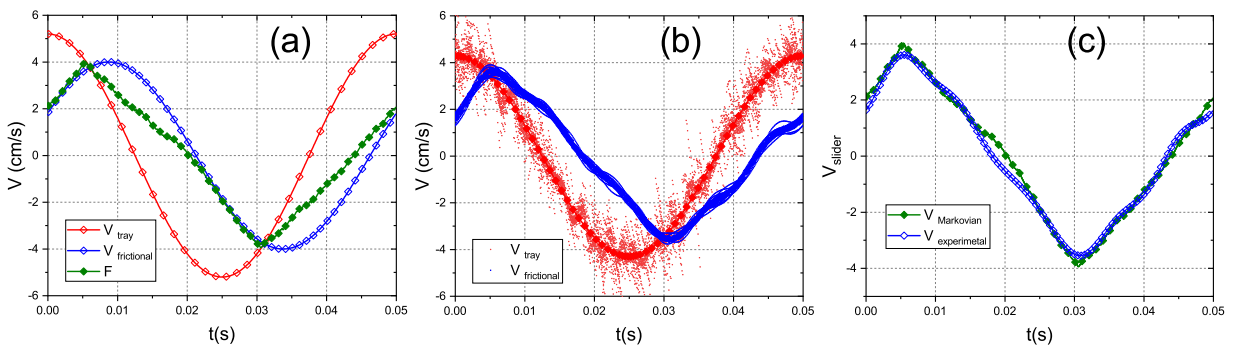


Fig. 7. Markovian model results: (a) Tray velocity and the linearly predicted slider velocity. The green symbol corresponds to the prediction of the Markovian model. (b) The same magnitudes calculated from the experimental data. (c) Experimental slider velocity and the velocity obtained from the Markovian model. (For interpretation of the references to color in this figure legend, the reader is referred to the web version of this article.)

The physical interpretation of this product χ is a threshold of likelihood to follow either of the attractor curves. It has the following properties: in the limit of vanishing χ the sliders velocity always coincides with the first attractor, no matter what value the random generator provides. In case $\chi > 1$, the sliders velocity always coincides with the second attractor, no matter what value the random generator provides. The critical parameters in determining what attractor to follow, just happen to be these two arguments χ_μ and χ_{acc} . Indeed, for zero acceleration, χ_{acc} vanishes, and the sliders velocity always coincides with the first attractor. Likewise, for infinite acceleration, χ_{acc} diverges, and the sliders velocity always coincides with the second attractor. An analogous requirement holds for the friction coefficients: for infinite static or vanishing dynamic coefficients, sliders velocity always coincides with the first attractor, while for equal friction coefficients there is no static coefficient effect, whence sliders velocity always coincides with the second attractor. The two Heaviside theta-functions of Eq. (7) grant the correct output of the algorithm.

As the velocity decays linearly with the dynamic friction coefficient, its decay to the equilibrium value should occur according to $v_{deceleration} = v_d - \mu_{dyn}gt$. When we use δt_{Markov} as the discrete Markovian time step, and δv_{Markov} as the discrete Markovian velocity step, the velocity-time aspect ratio remains unchanged upon requiring that $\delta v_{Markov} \equiv \mu_{dyn}g\delta t_{Markov}$. Then, the velocity jump is unity in the case of the first attractor, and a fraction $\text{rnd}[\mu_{dyn}/\mu_{stat}]$ smaller for the second attractor. Setting this ratio to unity (as it is in most experimental cases) does not lose the crucial information on the value of $\Delta\mu$, as it is numerically hardwired into χ .

In order not to confuse the reader, we did not yet comment on the exact value of t_{mx} we used to calculate the second attractor. Had we used the value prescribed by its definition $\mu_{dyn}gt_{mx} = |v_d|$, the phase delay of the second attractor would be one third the value we have used in our simulations.

6. Conclusion

We present experimental data of the motion of a macroscopic piece moving freely under the frictional interaction with a harmonically oscillating horizontal substrate. We observed that, despite plenty of uncontrolled parameters like the local heating due to friction, the existence of uncontrolled dust on the tray or a not perfectly polished slider surface, the dynamics displayed by the slider is periodic with a well-defined amplitude and phase delay

against the driving signal. The threshold acceleration, where the slider starts to move, is well defined and the resulting dynamics have the same periodicity. The transition between the stuck to the stick-free regime is discontinuous; all our experiments point towards a critical acceleration below which the slider is permanently stuck to the substrate. From the kinematic approach introduced to predict the sliders velocity, we deduce that –at least slightly beyond threshold– static friction operates via stick-and-loose stochastic process, which depends on slider's relative velocity and acceleration. This fact inspired the introduction of a Markovian process to model the competition between two attractor solutions. Under this simple assumption, the slider velocity can be very well predicted. Moreover, the authors are confident that the same model applies to all possible driver accelerations, as the model is built in such a way as to reproduce the correct extreme acceleration cases.

Acknowledgments

This work was partially funded by [Ministerio de Economía y Competitividad \(Spanish Government\)](#) through Projects No. FIS2014-57325.

References

- [1] Popova E, Popov VL. The research works of Coulomb and Amontons and generalized laws of friction. *Friction* 2015;3(2):183–90.
- [2] Amontons G. De la resistance causée dans les machines. *Mémoire de l'Académie RA* 1699:257–82.
- [3] de Coulomb C-A. *Théorie des machines simples en ayant égard au frottement de leurs parties et à la roideur des* (Éd.1821). Hachette Livre BNF; 2012.
- [4] Frank W D, Maarten P de B, James A K, E DRJr, Peggy J C, Martin L D. The role of van der waals forces in adhesion of micromachined surfaces. *Nat Mater* 2005;4:629.
- [5] Popp K, Stelter P. Stick-slip vibrations and chaos. *Philos Trans* 1990;332:89–105.
- [6] Popov V. What does friction really depend on? Robust governing parameters in contact mechanics and friction. *Phys Micromech* 2016;19:115–22.
- [7] Pennestrì E, Rossi V, Salvini P, Valentini PP. Review and comparison of dry friction force models. *Nonlinear Dyn* 2016;83(4):1785–801.
- [8] Berger E. Friction modeling for dynamic system simulation. *Appl Mech Rev* 2002;55:535–77.
- [9] Person B. *Sliding friction*. Springer-Verlag Berlin Heidelberg; 1998.
- [10] RP F, RB L, M S. *The feynman lectures on physics, 1*. Addison-Wesley; 1964.
- [11] N Gaus CP, Hetzler H. Determination of a stochastic friction coefficient depending on a randomly rough surface. *PAMM Proc Appl Math Mech* 2012;12:241–2.
- [12] Won Seok Kang CKC, Yoo HH. Stochastic modeling of friction force and vibration analysis of a mechanical system using the model. *J Mech Sci Technol* 2015;29:3645–52.